

Spectroscopic properties of Cr³⁺ ions at the defect sites in cubic fluoroperovskite crystals

Yu Wan-Lun, Zhang Xin-Min, Yang La-Xun, and Zen Bao-Qing

Department of Physics, Sichuan Normal University, Chengdu 610066, People's Republic of China

(Received 29 November 1993; revised manuscript received 28 April 1994)

The spin-Hamiltonian (SH) parameters for the ⁴A₂(F) state of 3d³/3d⁷ ions for tetragonal and trigonal symmetries are studied as a function of the crystal-field (CF) parameters based on simultaneous diagonalization of the electrostatic, CF, and the spin-orbit-coupling Hamiltonians. The results obtained are compared to those in earlier works. The CF and SH parameters of Cr³⁺ ions at the A and M vacancies and at codoped Li⁺ sites in the cubic fluoroperovskites AMF₃ are investigated by taking into account the contributions of the defects and the defect-induced lattice distortion. Suitable models are proposed for the lattice distortion, and the distortion parameters are obtained by adjusting them to fit to the observed data for the SH parameters and the energy of the first excited state.

I. INTRODUCTION

When Cr³⁺ impurities substitute for the divalent cations M²⁺ in cubic fluoroperovskite crystals AMF₃, various defect sites are formed owing to the charge compensation, including M vacancies (V_M), A vacancies (V_A), and codoped Li⁺ impurities (see Fig. 1).¹⁻⁶ One of the most important effects of such a defect appears in the spin Hamiltonian (SH), which shows parameter values quite different from those for the perfect cubic site. Thus electron paramagnetic resonance (EPR) and electron-nuclear double resonance (ENDOR) experiments have become powerful tools in the study of the defects.¹⁻⁶ Another effect is on the optical properties, in which additional optical fine-structure lines appear in the spectra.⁵⁻⁸ The latter effect has recently received much attention, especially in the valuable laser crystals Cr³⁺:KZnF₃ (Refs. 5, 7, 8) and Cr³⁺:RbCdF₃,⁶ where defect sites have been found to make important contributions to the laser transition bands.

Although a great deal of work has been devoted to experimental study of the defect centers, the present work performs a theoretical investigation. In Sec. II, the formalism and the origins of the crystal-field (CF) interaction are discussed for the defect centers, while in Sec. III the SH parameters are studied as a function of the CF parameters. The results are presented in Sec. IV and a summary is made in Sec. V.

II. CRYSTAL FIELDS

For the cubic site in Cr³⁺:AMF₃ crystals, the magnetic ion Cr³⁺ (3d³) is subject to a regular octahedral CF, which can be written as⁹

$$\mathcal{H}_{CF}(c) = B_{40}(c)C_0^{(4)} + B_{4m}(c)[C_m^{(4)} + (-1)^m C_{-m}^{(4)}], \quad (1)$$

with

$$D_{qc} = 2PB_{40}(c), \quad B_{40}(C) = QB_{4m}(c), \quad (2)$$

where C_q^(k) are the normalized spherical harmonics. The values of m, P, and Q depend on the choice of coordinate

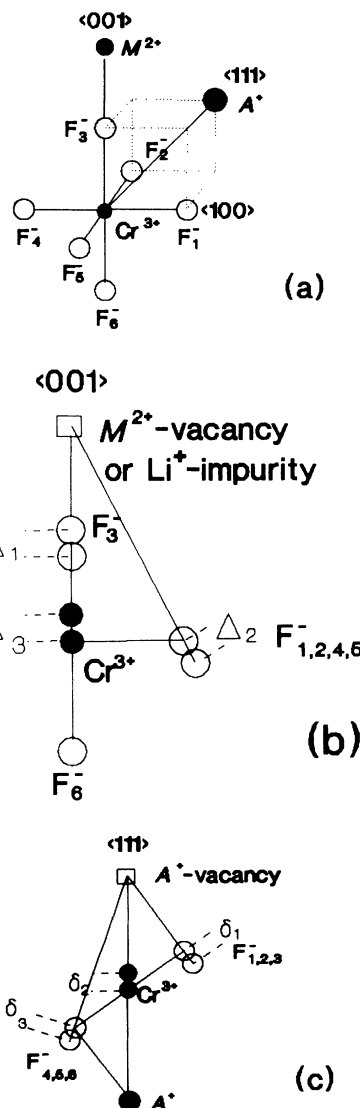


FIG. 1. Various sites in Cr³⁺:AMF₃. (a) Cubic Site, (b) tetragonal Cr³⁺-Li⁺ and Cr³⁺-V_M sites, and (c) a trigonal Cr³⁺-V_A site.

system: $m=4$, $P=\frac{1}{42}$, and $Q=\sqrt{\frac{14}{5}}$ when $z\|\langle 001 \rangle$ and $m=3$, $P=-\frac{1}{28}$, and $Q=\pm\sqrt{\frac{7}{10}}$ when $z\|\langle 111 \rangle$ (the signs are related to each other by a 60° rotation of the x and y axes around the z axis; see Ref. 9). Equation (2) defines the usually used cubic CF parameter D_{qc} , whose value depends on the Cr³⁺-F⁻ distance R_0 .

When a vacancy or a codoped impurity is presented in the neighborhood of the central metal ion, the point symmetry is changed from O_h to C_{4v} or C_{3v} , forming a defect center. The CF Hamiltonian can be expressed in a unifying form as⁹

$$\mathcal{H}_{CF} = B_{20}C_0^{(2)} + B_{40}C_0^{(4)} + B_{4m}[C_m^{(4)} + (-1)^m C_{-m}^{(4)}], \quad (3)$$

where $m=4$ for the C_{4v} -symmetric defect sites ($z\|\langle 001 \rangle$) and $m=3$ for the C_{3v} ones ($z\|\langle 111 \rangle$). It is clear that \mathcal{H}_{CF} is different from $\mathcal{H}_{CF}(c)$, owing to the effect of charge compensation, denoted by \mathcal{H}'_{CF} . Considering this, it can be written that

$$\mathcal{H}_{CF} = \mathcal{H}_{CF}(c) + \mathcal{H}'_{CF}, \quad (4)$$

where

$$\mathcal{H}'_{CF} = \tilde{B}_{20}C_0^{(2)} + \tilde{B}_{40}C_0^{(4)} + \tilde{B}_{4m}[C_m^{(4)} + (-1)^m C_{-m}^{(4)}].$$

The parameters \tilde{B}_{kq} represent the net charge compensation (NCC) effect on the CF for a defect center:

$$\begin{aligned} \tilde{B}_{20} &= B_{20}, \\ \tilde{B}_{40} &= B_{40} - B_{40}(c), \\ \tilde{B}_{4m} &= B_{4m} - B_{4m}(c). \end{aligned} \quad (5)$$

It is convenient to define⁹

$$\begin{aligned} D_q &= P(B_{40} + QB_{4m}) = D_{qc} + P(\tilde{B}_{40} + Q\tilde{B}_{4m}), \\ B'_{40} &= B_{40} - QB_{4m} = \tilde{B}_{40} - Q\tilde{B}_{4m}. \end{aligned} \quad (6)$$

The CF parameters B_{20} and B'_{40} vanish identically in cubic symmetry; they result entirely from the NCC effect for the defect sites, as can be seen from Eqs. (5) and (6). We will show in Sec. IV that the sign of the zero-field-splitting (ZFS) parameter changes with the inversion of the signs of these two CF parameters, for either tetragonal or trigonal symmetry.

The defect (a vacancy or a codoped impurity) must have a contribution to \tilde{B}_{km} because of the change of charge. The contribution is denoted by $\tilde{B}_{km}(D)$. Further, the crystalline lattice will be distorted owing to the presence of the defect, making an additional contribution to \tilde{B}_{km} , denoted by $\tilde{B}_{km}(\text{LD})$. Consequently, we write

$$\tilde{B}_{km} = \tilde{B}_{km}(D) + \tilde{B}_{km}(\text{LD}). \quad (7)$$

We adopt the superposition model¹⁰ to obtain $\tilde{B}_{km}(\text{LD})$:

$$\begin{aligned} \tilde{B}_{km}(\text{LD}) &= f_k \bar{A}_k(R_0) (-1)^m \sum_L [(R_0/R_L)^{t_k} C_{-m}^{(k)}(\Theta_L, \Phi_L) \\ &\quad - C_{-m}^{(k)}(\Theta_L^c, \Phi_L^c)], \end{aligned} \quad (8)$$

with $f_2=2$ and $f_4=8$ (Refs. 10, 11) and the summation is over all ligands. $\bar{A}_k(R_0)$ ($k=2,4$) are intrinsic param-

eters and t_k the power-law exponents.¹⁰ The coordinates are denoted by (R_L, Θ_L, Φ_L) for a ligand in the defect cluster, and by $(R_L^c, \Theta_L^c, \Phi_L^c)$ for a ligand in the cubic cluster. The reference distance has been taken as the Cr-F distance R_0 in the cubic site.

In order to calculate $\tilde{B}_{km}(\text{LD})$ for the defect centers, one must assume a reasonable lattice distortion model for the Cr³⁺-6F⁻ cluster. Let us first consider a Cr³⁺- V_M center in Cr³⁺:AMF₃ crystals [see Fig. 1(b)]. Considering an M^{2+} vacancy as an effective negative charge of $-2e$, the F⁻ ion in the $\langle 001 \rangle$ axis [F(3) in Fig. 1(b)] will move toward the central magnetic ion Cr³⁺, by an amount Δ_1 . Further, the four planar F⁻ ions [F(1), F(2), F(4), and F(5) in Fig. 1(b)] may move away from the vacancy along lines linking the vacancy and these anions, although the displacement, denoted by Δ_2 , should be less than Δ_1 . Meanwhile, the Cr³⁺ can move towards the vacancy. The movement Δ_3 of Cr³⁺ could not be considerably greater than Δ_1 since F(3) is closer to the vacancy than Cr³⁺. This lattice distortion model is supported by the calculation published by Yeung¹² for the Cr³⁺- V_{Mg} center in MgO crystal, which is quite similar to our case. His results, obtained by using the lattice relaxation model¹³ and by assuming the same set of force parameters for the MgO lattice, can be expressed as $\Delta_1 \approx 0.03R_0$, $\Delta_2 \approx 0.02R_0$, $\Delta_3 \approx 0.05R_0$, and $R_0 \approx 1.927 \text{ \AA}$. The Cr³⁺-Li⁺ centers are considered in the same way, except that a codoped Li⁺ impurity serves an effective charge of $-e$.

The Cr³⁺- V_A centers can be treated in a similar way [see Fig. 1(c)]. Since an A^+ vacancy serves as an effective charge of $-e$, the three "front" (F(1), F(2), and F(3)) and three "back" (F(4), F(5), and F(6)) F⁻ ions will move away from the vacancy, by amounts of δ_1 and δ_3 , respectively. On the other hand, the central magnetic ion may move toward the vacancy; the displacement is denoted by δ_2 . The net effect for the assumed displacements of the central metal ion and the ligands appears as an outward rotation of the front F⁻ ions by an angle α and an inward rotation of the back F⁻ ions by β around the $\langle 111 \rangle$ axis, as has been observed from ENDOR experiments for the Fe³⁺- V_k center in KZnF₃ crystal.¹⁴

When the superposition model is extended to the next-nearest-neighbor ions (cations) to calculate $\tilde{B}_{kq}(D)$, one will encounter both conceptual and technical problems. The conceptual problem arises from the assumption of this model that the CF parameters come entirely from the nearest-neighbor ligands.¹⁰ However, from the electrostatic point of view, the defect must contribute to the CF parameters. The technical problem is what the signs and magnitudes of the phenomenological parameters \bar{A}_k and t_k are for the various kinds of defects. On the other hand, since the defect is distant from the central metal ion, the interaction between the defect and the open-shell $3d^3$ electrons of the central metal ion should be mainly electrostatic, and the short-range (i.e., the overlap and covalency) effects should be negligible.¹⁰ Thus it seems reasonable to adopt the point-charge model in the calculation of $\tilde{B}_{kq}(D)$:

$$\tilde{B}_{km}(D) = -eq_D \langle r^k \rangle_{3d} R_D^{-(k+1)} (-1)^m C_{-m}^{(k)}(\Theta_D, \Phi_D), \quad (9)$$

where (R_D, Θ_D, Φ_D) are the coordinates of the defect and q_D is the effective charge of the defect. The expectation values $\langle r^2 \rangle_{3d} = 1.435$ a.u. and $\langle r^4 \rangle_{3d} = 4.264$ a.u. (Ref. 15) as well as the data for the $M^{2+}-F^-$ distance R_H of the host lattice (Ref. 16) will be used in our calculations.

It is expected that $R_0 < R_H$ in $Cr^{3+}:AMF_3$ crystals because of the smaller size of Cr^{3+} and the net positive charge e when a Cr^{3+} replaces M^{2+} . Also the values of R_0 will vary from one crystal to another, but we are unable to determine them in this work. Nevertheless, it seems reasonable to estimate R_0 in the range 1.9–2.0 Å, noting that $R_H = 2.0$ –2.4 Å for these crystals (see Ref. 16) and 1.9 Å for chromium fluorides.¹⁷ However, we can avoid most of the difficulty caused by the lack of the exact values of R_0 in the calculations of CF parameters B_{km} by taking R_0 as the reference distance of the superposition model, $\bar{A}_k(R_0)$ as adjustable parameters (see below for details), and R_L (or, equivalently, Δ_i and δ_i) in units of R_0 . The assumption that $R_0 = R_H$ is made when we have to use the exact values of R_0 , without significant change of the final results for the lattice distortion, which are therefore expressed as Δ_i/R_0 and δ_i/R_0 .

The superposition-model power-law exponents are taken as $t_2 = 3$ and $t_4 = 5$ for all cases, considering the highly ionic nature of the crystals.¹⁰ The values of the intrinsic parameter $\bar{A}_4 \equiv \bar{A}_4(R_0)$ are obtained using the relationship $\bar{A}_4 = \frac{3}{4} D_{qc}$ (Ref. 9), with D_{qc} values derived from reported optical data. In addition, $\bar{A}_2 \equiv \bar{A}_2(R_0)$ is taken to be $10.8 \bar{A}_4$, considering that the ratio \bar{A}_2/\bar{A}_4 tends to be constant and in the range 10–12 for iron-group ions.^{11,18,19}

III. SPIN-HAMILTONIAN PARAMETERS

The SH is given as ($S = \frac{3}{2}$)

$$\mathcal{H}_S = \beta g_{\parallel} H_z S_z + \beta g_{\perp} (H_x S_x + H_y S_y) + \frac{1}{3} b_2^0 O_2^0 \quad (10)$$

for both C_{4v} and C_{3v} symmetries. In cubic symmetry, $g_{\parallel} = g_{\perp} = g_c$ and $b_2^0 = 0$. Thus the values of $g' = g_{\perp} - g_{\parallel}$, $g_{\parallel} - g_c$, and b_2^0 for a defect site in $Cr^{3+}:AMF_3$ represent the NCC contribution to the SH parameters. Rudowicz^{20,21} has proposed the NCC model to extract the net contribution to the zero-field-splitting parameters due to charge compensation; the proposed model has been successfully applied to various defect centers for Cr^{3+} , Fe^{3+} , and Gd^{3+} in $A_2MX_4^-$, AMX_3^- , and MX_2 -type crystals.

The parameters g_{\parallel} , g_{\perp} , and b_2^0 appearing in the effective Hamiltonian (10), as well as the energies of excited states, are related to the actual Hamiltonians, namely the CF and the spin-orbit (SO) coupling. Under the action of the Hamiltonians, the ground state ${}^4A_2(F)$ is split into two Kramers doublets $\Psi_g(E'\gamma)(\gamma = \alpha', \beta')$ and $\Psi_g(E''\gamma)(\gamma = \alpha'', \beta'')$, which can be expressed as ($\Gamma = E', E''$ for either C_{4v} or C_{3v})

$$\Psi_g(\Gamma\gamma) = \sum_{\alpha SL} C_{\alpha SL\Gamma\gamma} |3d^3 \alpha SL \Gamma\gamma\rangle, \quad (11)$$

where α denotes repeating representations. In order to obtain the mixing coefficients $C_{\alpha SL\Gamma\gamma}$ and the energies of

$\Psi_g(\Gamma\gamma)$, we diagonalize the electrostatic interaction, CF, and SO simultaneously within the $3d^3$ configuration. The parameter b_2^0 is then obtained by using the well-known relation

$$2b_2^0 = E[\Psi_g(E'')] - E[\Psi_g(E')]$$

(Refs. 22–24). Since the g factors describe the first-order effect of an external magnetic field \mathbf{H} on the ground state ${}^4A_2(F)$, in calculation of them we treat the Zeeman in-

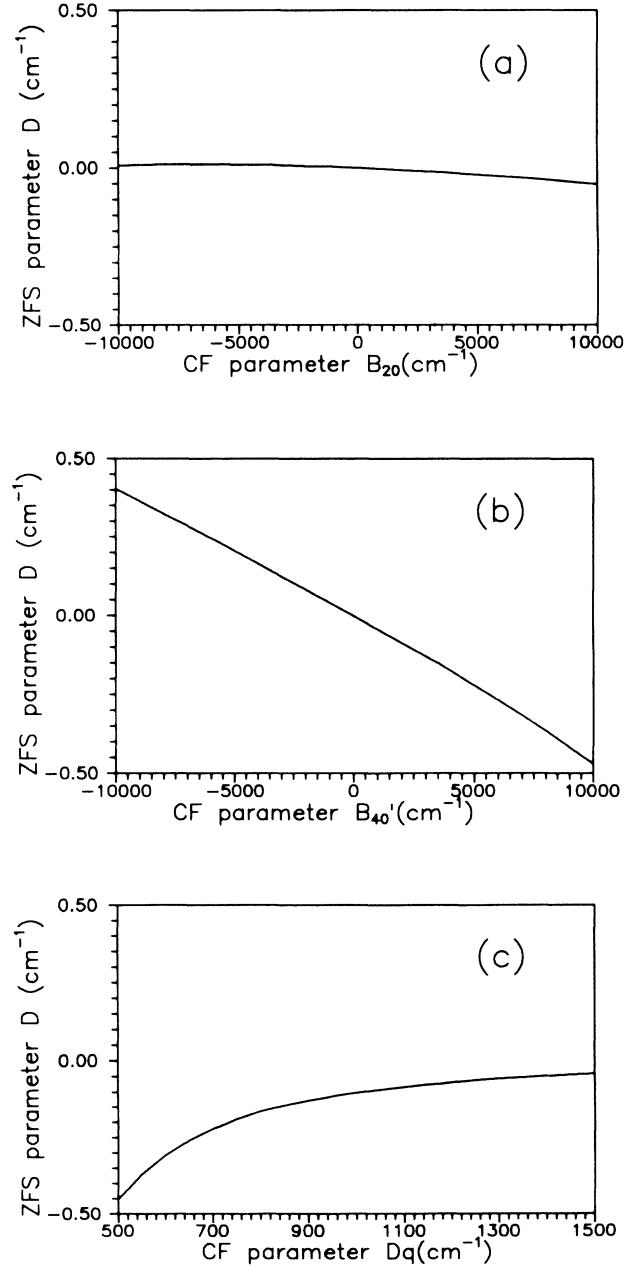


FIG. 2. ZFS parameter $D = b_2^0$ for a ${}^4A_2(d^{3,7})$ -state ion in tetragonal symmetry vs (a) $B_{20}(B_{40}' = 0, D_q = 1400 \text{ cm}^{-1})$, (b) $B_{40}'(B_{20} = 0, D_q = 1400 \text{ cm}^{-1})$, and (c) $D_q(B_{20} = 2000 \text{ cm}^{-1}, B_{40}' = 1000 \text{ cm}^{-1})$; $B = 800 \text{ cm}^{-1}$, $C = 3000 \text{ cm}^{-1}$, $\alpha = 0$, and $\zeta = 246 \text{ cm}^{-1}$.

teraction as a perturbation, which is written as²⁵

$$\mathcal{H}_{\text{Zeeman}} = \beta \left[\sum_i s_i + k \sum_i l_i \right] \cdot \mathbf{H}. \quad (12)$$

The g factors are then given as

$$g_{\parallel} = 2 \langle \Psi_g(E'\alpha') \left| \sum_i [s_{zi} + kl_{zi}] \right| \Psi_g(E'\alpha') \rangle, \quad (13)$$

$$g_{\perp} = \langle \Psi_g(E'\beta') \left| \sum_i [s_{xi} + kl_{xi}] \right| \Psi_g(E'\alpha') \rangle.$$

The parameter k is the orbital reduction factor describing the covalency and overlap effects on the orbital angular momentum l_i .²⁵

We construct the basis functions $|3d^3\alpha SL\Gamma\gamma\rangle$ and calculate the matrix elements of the electrostatic, CF, and SO interactions by using the intermediate CF coupling scheme, which has been proposed by König and Schnakig²⁶⁻²⁸ and described recently in the form of the irreducible tensor operator technique by Yu and Rudowicz.²⁹ The reduction matrix elements tabulated in Ref. 30 have been used. The Hamiltonian matrices obtained are 39×39 (E') and 21×21 (E'') dimensional for

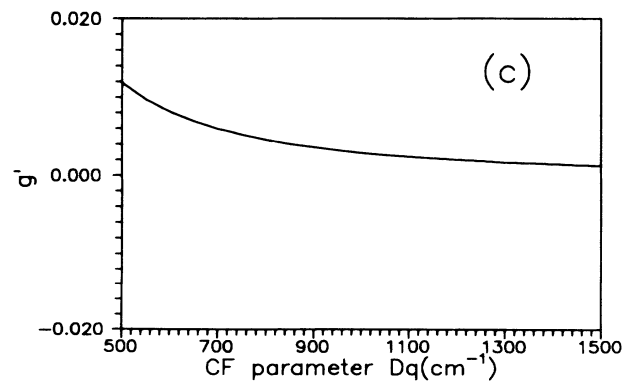
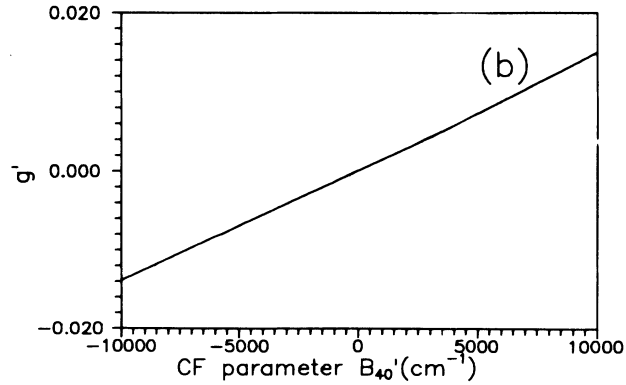
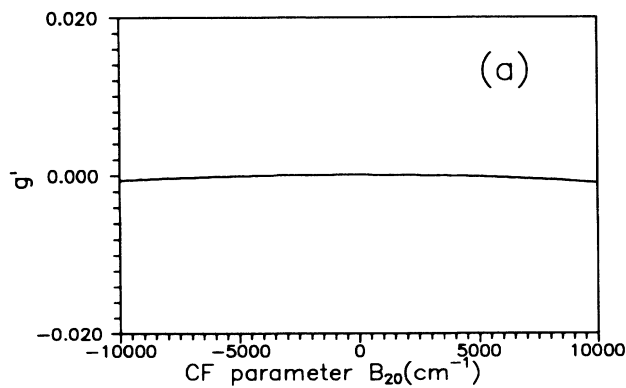


FIG. 3. Zeeman parameter $g' = g_{\perp} - g_{\parallel}$ for a ${}^4A_2(d^{3,7})$ -state ion in tetragonal symmetry vs (a) B_{20} , (b) B'_{40} , and (c) D_q . Values of the parameters are as in Fig. 2; $k = 1$.

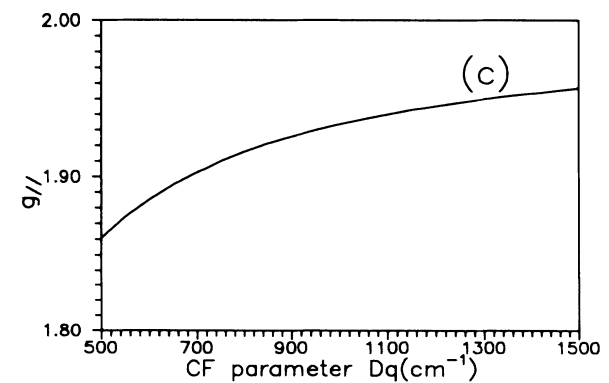
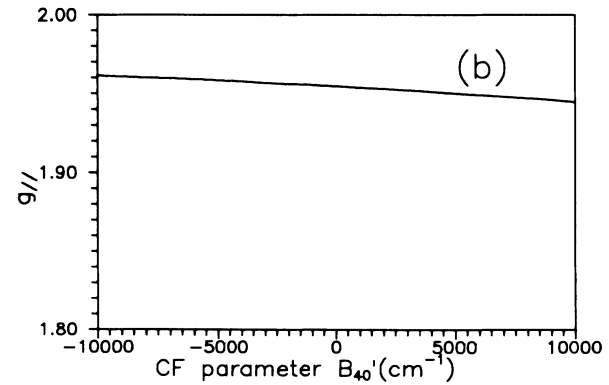
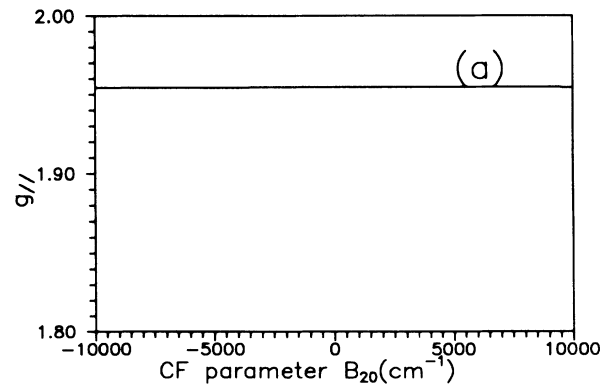


FIG. 4. Zeeman parameter g_{\parallel} for a ${}^4A_2(d^{3,7})$ -state ion in tetragonal symmetry vs (a) B_{20} , (b) B'_{40} , and (c) D_q . Values of the parameters are as in Fig. 2; $k = 1$.

C_{3v} and both 30×30 (E' and E'') for C_{4v} . The calculations for the matrices and the diagonalization of them, as well as the calculations of SH parameters for both symmetries, are carried out using a FORTRAN program. Hence the SH parameters and the energies of excited states can be obtained as a function of the CF parameters B_{20} , B'_{40} , and D_q , the Racah electrostatic parameters B and C , the Trees correction α , the SO coupling constant ζ , and the orbital reduction factor k for either of the symmetries. The program is also applicable to such groups as D_{3d} , D_3 , D_{2d} , D_4 , and D_{4h} isomorphic to C_{3v} or C_{4v} .

As has been mentioned in Sec. II, the parameters B_{20} and B'_{40} serve as a measurement of the departure of a tetragonal or trigonal CF Hamiltonian from the cubic one. For the defect centers under study, these parameters arise entirely from the NCC effect [see Eqs. (5) and (6)]. On the other hand, we have $b_2^0 = 0$ and $g' = 0$ for the cubic centers. Therefore the NCC effect on the SH parameters is just a result of the NCC effect on the CF. We are now interested in the dependencies of the SH parameters on the CF ones B_{20} , B'_{40} , and D_q , which are plotted in Figs. 2–4 for tetragonal symmetry and in Figs. 5–7 for

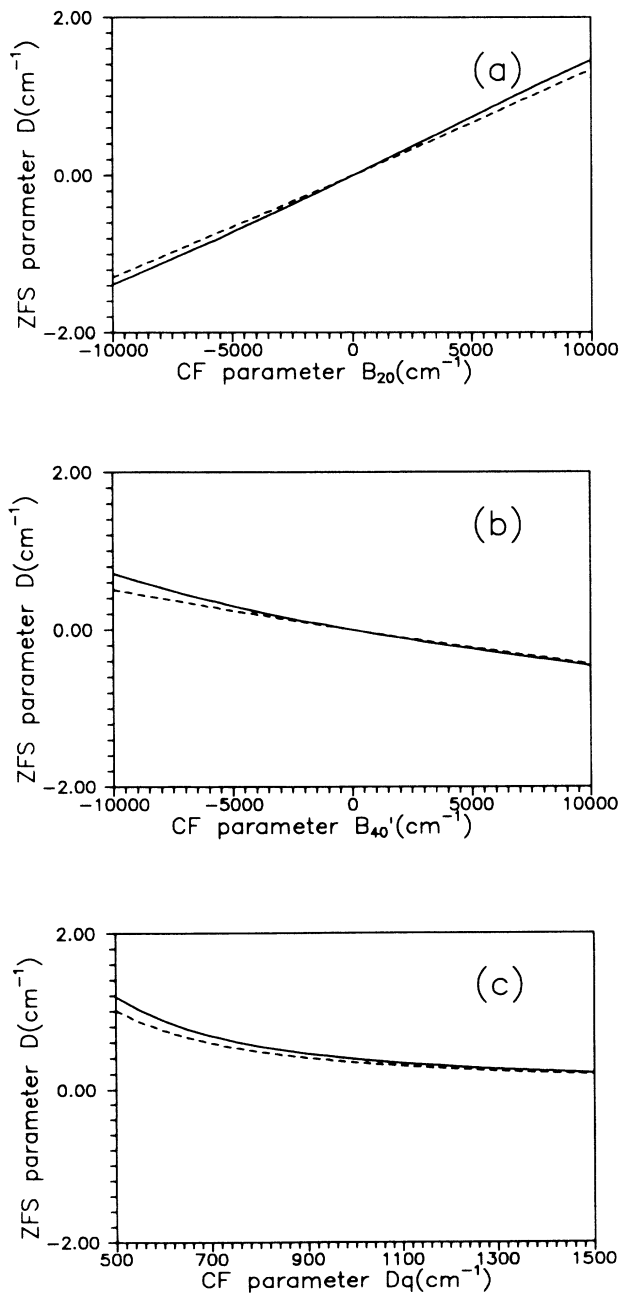


FIG. 5. ZFS parameter $D = b_2^0$ for a ${}^4A_2(d^{3,7})$ -state ion in trigonal symmetry vs (a) B_{20} , (b) B'_{40} , and (c) D_q . Values of the parameters are as in Fig. 2. Solid lines, the present work; dashed lines, Ref. 22.

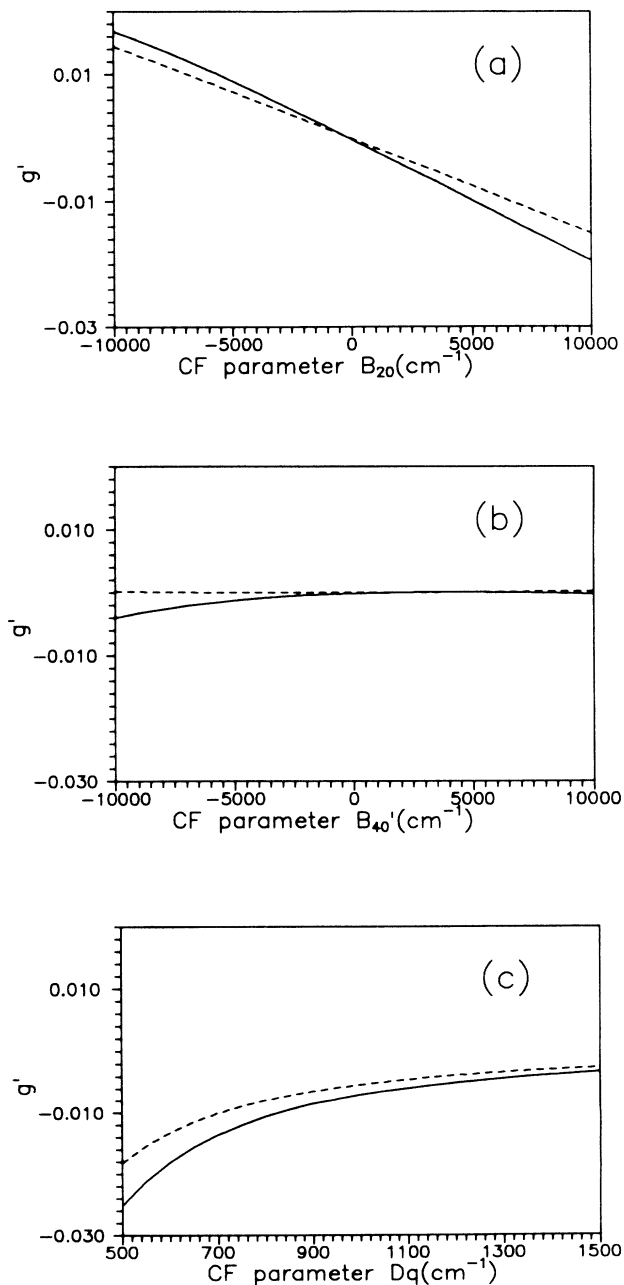


FIG. 6. Zeeman parameter $g' = g_{\perp} - g_{\parallel}$ for a ${}^4A_2(d^{3,7})$ -state ion in trigonal symmetry vs (a) B_{20} , (b) B'_{40} , and (c) D_q . Values of the parameters are as in Fig. 2; $k = 1$. Solid lines, the present work; dashed lines, Ref. 23.

trigonal symmetry. It is noted that B_{20} is of little importance for the SH parameters in tetragonal symmetry. In either of the symmetries, b_2^0 and g' become zero at $B_{20}=B'_{40}=0$, as expected. Further, they both reverse signs when B_{20} and B'_{40} change in sign. According to the superposition model (Ref. 10), B_{20} and B'_{40} change in sign when the structure of a crystal of D_{4h} , D_{2d} , and D_{3d} symmetry goes from compression to elongation. Hence the calculated results indicate opposite signs of b_2^0 and g' for compressive and elongated crystals of these symmetries.

The results for trigonal symmetry are compared to

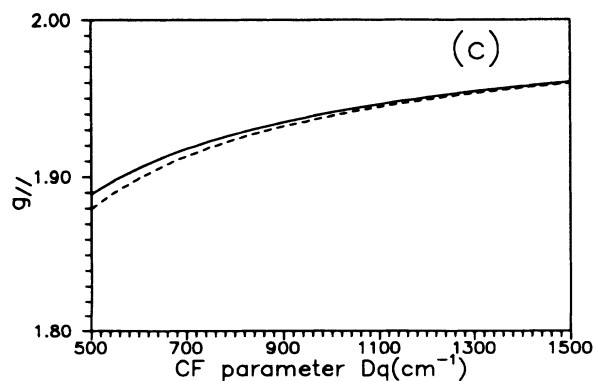
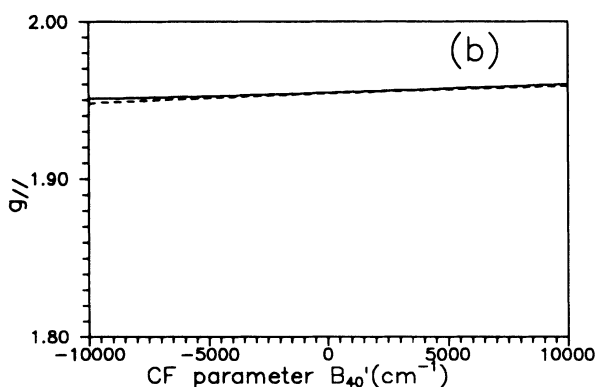
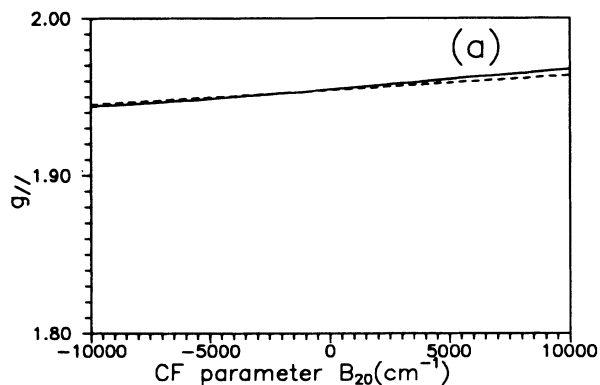


FIG. 7. Zeeman parameter g_{\parallel} for a ${}^4A_2(d^{3,7})$ -state ion in trigonal symmetry vs (a) B_{20} , (b) B'_{40} , and (c) D_q . Values of the parameters are as in Fig. 2; $k=1$. Solid lines, the present work; dashed lines, Ref. 23.

those obtained by Macfarlane,^{22,23} as also shown in Figs. 5–7. The ranges of values of B_{20} and B'_{40} are chosen as $[-10000 \text{ cm}^{-1}, 10000 \text{ cm}^{-1}]$, corresponding to zero, weak, and intermediate distortion of crystals, while the range of D_q is chosen as $[500 \text{ cm}^{-1}, 1500 \text{ cm}^{-1}]$ corresponding to weak and intermediate strengths of the CF. The perturbation technique used by Macfarlane in the calculation of b_2^0 considers the cubic part of the CF and the diagonal part of the electrostatic interaction (in the strong CF scheme²⁵) as the unperturbed Hamiltonian, and the remaining parts of the CF and electrostatic interaction as the perturbed terms, together with the SO coupling. The Zeeman term was regarded as an additional perturbation Hamiltonian when calculating the g factors.²³ This technique has been suggested independently by Zdanski²⁴ for ${}^4A_2(3d^{3,7})$ - and ${}^3A_2(3d^{2,8})$ -state ions and applied to ${}^6S(3d^5)$ -state ions by Yu^{31,32} and Yu and Tan.³³ The perturbation expressions obtained by Macfarlane^{22,23} for the SH parameters of ${}^4A_2(3d^{3,7})$ ions in trigonal symmetry have frequently been adopted (e.g., Ref. 34), but there has been no independent justification of these expressions. The expressions have been formulated in terms of the conventional CF parameters Δ , v , and v' , related to those used in the present work by

$$\begin{aligned} B_{20} &= v - 2\sqrt{2}v', \\ B'_{40} &= (9/5)[v + (3/\sqrt{2})v'], \\ D_q &= \Delta/10 - (13/420)[v + (3/\sqrt{2})v']. \end{aligned} \quad (14)$$

By comparison one can see that Macfarlane's expressions^{22,23} work well indeed, especially for the cases of small B_{20} and B'_{40} and large D_q . Since our calculations are based on simultaneous diagonalization, our work provides a justification of Macfarlane's expressions.^{22,23}

IV. RESULTS

It follows from the discussions presented in Secs. II and III that the SH parameters are related to the lattice distortion parameters Δ_i and δ_i for the defect center in $\text{Cr}^{3+}:\text{AMF}_3$ crystals. However, before making numerical calculations, we need values of the parameters B , C , α , D_{qc} , ζ , and k . The SO coupling constant ζ has been calculated to be 246 cm^{-1} .³⁵ The former four parameters have been obtained for some crystals from optical data. Altshler and Larionov⁷ have observed the absorption spectra for $\text{Cr}^{3+}:\text{KZnF}_3$ and obtained $B=820$, $C=2900$, $D_{qc}=1500$, and $\alpha=80$, in cm^{-1} , for the cubic sites. The D_{qc} value was obtained mainly from the transition ${}^4A_2(F) \rightarrow {}^4T_2(F)$, which yields $10D_{qc}$ directly. However, owing to the phonon sidebands, the value given by the center of the optical transition band is actually somewhat greater than the real value of $10D_{qc}$. It is noted that the ${}^4T_2(F)$ state will be split into Γ_6 , Γ_7 , Γ_8 , and Γ'_8 under the action of the SO coupling.⁸ Among these, the lowest state Γ_7 has been observed to be 14091 cm^{-1} .^{5,8} The energy of this state, denoted by E_1 , can be expressed approximately as $10D_{qc} - 5\zeta/12$ to first order, neglecting the Jahn-Teller effect.⁸ By using $\zeta=246 \text{ cm}^{-1}$,³⁵ we ob-

TABLE I. Lattice distortion, CF, and SH parameters for tetragonal defect centers in $\text{Cr}^{3+}:\text{AMF}_3$ crystals.

	$\text{KZnF}_3\text{-V}_{\text{Zn}}$	$\text{KZnF}_3\text{-Li}^+$	$\text{RbCdF}_3\text{-V}_{\text{Cd}}$	$\text{RbCdF}_3\text{-Li}^+$	$\text{KCdF}_3\text{-V}_{\text{Cd}}$	$\text{KCdF}_3\text{-Li}^+$	$\text{CsCdF}_3\text{-V}_{\text{Cd}}$	$\text{CsCdF}_3\text{-Li}^+$
R_H (Å)	2.027	2.027	2.200	2.200	2.145	2.145	2.232	2.232
T (K)	300	300	300	300	492	492	300	300
k	0.62	0.62	0.63	0.63	0.63	0.63	0.63	0.63
$\Delta_1(R_0)$	0.0142	0.0147	0.0149	0.0227	0.0123	0.0178	0.0173	0.0273
$\Delta_2(R_0)$	0.0018	0.0018	0.0018	0.0018	0.0018	0.0018	0.0018	0.0018
$\Delta_3(R_0)$	0.028	0.03	0.03	0.03	0.03	0.03	0.03	0.03
B_{20} (cm^{-1})	3048.1	2447.6	2760.1	2832.7	2644.2	2483.8	2902.4	3185.2
B'_{40} (cm^{-1})	1073.8	1097.0	1059.4	1459.3	929.2	1194.0	1184.2	1717.3
D_q (cm^{-1})	1434.3	1434.1	1353.9	1363.4	1350.8	1357.1	1356.8	1369.5
b_0^2 (cm^{-1})	-0.0521	-0.0509	-0.0571	-0.0744	-0.0511	-0.0622	-0.0629	-0.0860
g_{\parallel}	1.9727	1.9727	1.9704	1.9704	1.9704	1.9704	1.9704	1.9705
g_{\perp}	1.9736	1.9736	1.9714	1.9718	1.9713	1.9715	1.9715	1.9720
E_1 (cm^{-1})	14015	14010	13244	13247	13242	13247	13245	13248
b_0^2 (cm^{-1})	-0.05421(5) ^a	-0.05080(5) ^a	-0.05693(5) ^a	Experiments	-0.05113(5) ^a	-0.06212(5) ^a	-0.06293(5) ^a	-0.08588(5) ^a
	-0.0522(4) ^b		-0.05690(5) ^c	-0.07439(5) ^a			-0.06286(5) ^c	
	-0.05409(5) ^d		-0.0722 ^e					
g_{\parallel}	1.9720(3) ^a	1.9723(3) ^a	1.9705(3) ^a	1.9702(3) ^a	1.9705(3) ^a	1.9711(3) ^a	1.9699(3) ^a	1.9698(3) ^a
	1.9718(4) ^b		1.9701(8) ^c				1.9696(8) ^c	
	1.9757(8) ^d		1.970 ^e					
g_{\perp}	1.9742(3) ^a	1.9736(3) ^a	1.9726(3) ^a	1.9728(3) ^a	1.9723(3) ^a	1.9729(3) ^a	1.9720(3) ^a	1.9728(3) ^a
	1.9741(6) ^b		1.9725(10) ^c				1.9722(10) ^c	
	1.9785(10) ^d		1.972 ^e					
E_1 (cm^{-1})	14016 ^{e,f}		13243 ^e					

^aReference 4.^bReference 3.^cReference 2.^dReference 1.^eReference 6.^fReference 5.

tain $D_{gc} = 1420 \text{ cm}^{-1}$, which is 80 cm^{-1} less than the value obtained from the absorption spectra. Similarly we obtain $D_{gc} = 1340 \text{ cm}^{-1}$ for RbCdF₃ from the experimental value $E_1 = 13303 \text{ cm}^{-1}$.⁶ This value, again 80 cm^{-1} less than the absorption spectra value (1420 cm^{-1}),⁶ as well as $B = 800 \text{ cm}^{-1}$, $C = 3290 \text{ cm}^{-1}$, and $\alpha = 0$,⁶ are adopted in the calculations also for Cr³⁺:KCdF₃ and Cr³⁺:CsCdF₃ crystals, whose optical data, to the best of our knowledge, are not available.

The orbital reduction factor k depends on the overlap of the orbitals of the central metal ion and the ligands,²⁵ and it is treated as an adjustable parameter as is usually done in the literature (e.g., Ref. 23). It has been taken as 0.7 for Cr³⁺ ions in oxides.²³ It is taken as 0.62–0.63 for Cr³⁺:AMF₃ in our calculations of the g factors. These values can be justified for the cubic center of Cr³⁺:KMgF₃, for which $g_c = 1.9733 \pm 0.0002$.³⁶ In fact, using $B = 823 \text{ cm}^{-1}$, $C = 3005 \text{ cm}^{-1}$, $\alpha = 85 \text{ cm}^{-1}$ (Ref. 7) and $D_{gc} = 1452 \text{ cm}^{-1}$ (80 cm^{-1} less than the absorption spectra value 1532 cm^{-1} given by Ref. 7), g_c is calculated as 1.9736 taking $k = 0.62$ and as 1.9731 taking $k = 0.63$; both values are consistent with the experimental value.

The energy of Γ_7 of ${}^4T_2(F)$, E_1 , will change under the action of the low-symmetric CF induced by the charge compensation for a defect center in Cr³⁺:AMF₃ crystals. It is thus a function of Δ_i or δ_i , like the SH parameters g_{\parallel} , g_{\perp} , and b_2^0 . We adjust Δ_1 , Δ_2 , and Δ_3 for tetragonal centers, whereas δ_1 , δ_2 , and δ_3 for trigonal ones, to fit to the experimental values of these parameters. The results obtained are given in the Tables I and II.

It should be pointed out that defect-induced lattice distortion plays a major role in affecting the SH parameters for either the tetragonal or the trigonal centers. For example, for the Cr³⁺-V_{Zn} center in a Cr³⁺:KZnF₃ crystal, omitting the lattice distortion, b_2^0 is calculated to be -0.0078 cm^{-1} , i.e., one order of magnitude less than the experimental data^{1,3,4} listed in Table I. For the trigonal Cr³⁺-V_K center in KZnF₃, similarly we obtain $b_2^0 = 0.1547 \text{ cm}^{-1}$, which is even opposite in sign to the experimental value (-0.1613 cm^{-1} , see Table II).

The results obtained for the lattice distortion indicate $\Delta_1 \gg \Delta_2 > 0$ and $\delta_1 \gg \delta_3 > 0$, as expected. The results for the Cr³⁺-V_M centers in AMF₃ are compared with $\Delta_1 \approx 0.03R_0$, $\Delta_2 \approx 0.02R_0$, and $\Delta_3 \approx 0.05R_0$ which can be derived from Ref. 12 (Table I) for Cr³⁺-V_{Mg} in MgO crystal. It is also noted that the results for the Cr³⁺-V_K center in KZnF₃:Cr³⁺, which can be alternatively expressed as $\alpha = 2.6^\circ$ and $\beta = 1.7^\circ$, are comparable to $\alpha = 2.8 \pm 0.3^\circ$ and $\beta = 1.1 \pm 0.3^\circ$ observed for the Fe³⁺-V_K center in KZnF₃ crystal.¹⁴ Since Cr³⁺ and Fe³⁺ have the same charge and a close ionic radius (0.63 \AA for Cr³⁺ and 0.64 \AA for Fe³⁺), the results may be considered reasonable.

TABLE II. Lattice distortion, CF, and SH parameters for trigonal defect centers in Cr³⁺:AMF₃ crystals.

	KZnF ₃ -V _k	RbCdF ₃ -V _{Rb}
R_H (Å)	2.027	2.200
T (K)	300	300
k	0.62	0.63
$\delta_1(R_0)$	0.02	0.0185
$\delta_2(R_0)$	0.03	0.03
$\delta_3(R_0)$	0.01	0.01
B_{20} (cm ⁻¹)	-787	-775
B_{40}^2 (cm ⁻¹)	863	746
D_g (cm ⁻¹)	1369	1294
b_2^0 (cm ⁻¹)	-0.1646	-0.1577
g_{\parallel}	1.9716	1.9693
g_{\perp}	1.9725	1.9703
E_1 (cm ⁻¹)	13 742	12 972
	Experiments	
b_2^0 (cm ⁻¹)	-0.1613(5) ^a	-0.1576 ^b
g_{\parallel}	1.9716(5) ^a	1.969(1) ^b
g_{\perp}	1.9725(4) ^a	1.971(1) ^b
E_1 (cm ⁻¹)	13 765 ^c	13 004 ^b

^aReference 3.

^bReference 6.

^cReference 5.

V. SUMMARY

We have made an investigation of the SH parameters and the energy of the first excited state for Cr³⁺-V_M, Cr³⁺-V_A, and Cr³⁺-Li defect centers in selected cubic AMF₃ lattices using available experimental data. The contribution arising from the defect itself has been taken into account in calculating the NCC effect on CF and SH parameters. This contribution has been shown to be non-negligible in the trigonal centers, although the main source comes from the defect-induced lattice distortion in both the tetragonal and trigonal centers. The models and method used in this paper are applicable to other cases. In addition, we have studied the SH parameters as a function of CF parameters for ${}^4A_2(3d^{3,7})$ ions in tetragonal and trigonal symmetries, based on simultaneous diagonalization of electrostatic, CF, and SO Hamiltonians. The results have been used to justify Macfarlane's perturbation expressions which have been frequently adopted in the literature.

ACKNOWLEDGMENTS

This work has been supported by the National Education Committee of P. R. China. One of the authors (X. M. Zhang) would like to thank the Science and Technology Committee of Yun-Lan Province for financial support.

¹M. Binos, A. Leble, J. J. Rousseau, and J. C. Fayet, J. Phys. (Paris) Colloq. **34**, C9-285 (1973).

²J. J. Rousseau, Y. Gesland, M. Binos, and J. C. Fayet, C. R. Acad. Sci. Ser. B **279**, 103 (1974).

³J. L. Patel, J. J. Davies, B. C. Vavenett, H. Takeuchi, and K. Horai, J. Phys. C **9**, 129 (1976).

⁴H. Takeuchi and M. Arakawa, J. Phys. Soc. Jpn. **53**, 376 (1984).

- ⁵Y. Vaills, J. Y. Buzaré, and M. Rousseau, *J. Phys. Condens. Matter* **2**, 3997 (1990).
- ⁶B. Villacampa, J. C. González, R. Alcalá, and P. J. Alonso, *J. Phys. Condens. Matter* **3**, 8281 (1991).
- ⁷N. S. Altshler and A. L. Larionov, *Opt. Spectrosc. (USSR)* **66**, 61 (1989).
- ⁸O. Pilla, E. Galvanetto, M. Montagna, and G. Viliani, *Phys. Rev. B* **38**, 3477 (1988).
- ⁹W. L. Yu and M. G. Zhao, *Phys. Rev. B* **37**, 9254 (1988).
- ¹⁰D. J. Newman and Betty Ng, *Rep. Prog. Phys.* **52**, 699 (1989).
- ¹¹A. Edgar, *J. Phys. C* **9**, 4304 (1976).
- ¹²Y. Y. Yeung, *J. Phys. Condens. Matter* **2**, 2461 (1990).
- ¹³Y. Y. Yeung and D. J. Newman, *J. Phys. C* **21**, 537 (1988).
- ¹⁴J. J. Krebs and R. K. Jeck, *Phys. Rev. B* **5**, 3499 (1972).
- ¹⁵S. Fraga, K. M. S. Saxena, and J. Karwowski, *Handbook of Atomic Data* (Elsevier, New York, 1976).
- ¹⁶M. Moreno, *J. Phys. Chem. Solids* **51**, 835 (1990).
- ¹⁷J. Emery and J. C. Fayet, *Solid State Commun.* **37**, 971 (1981).
- ¹⁸D. J. Newman, D. C. Pryce, and W. A. Runciman, *Am. Mineral.* **63**, 1278 (1978).
- ¹⁹Y. Y. Yeung and D. J. Newman, *Phys. Rev. B* **34**, 2258 (1986).
- ²⁰C. Rudowicz, *Solid State Commun.* **65**, 631 (1988).
- ²¹C. Rudowicz, *Phys. Rev. B* **37**, 27 (1988).
- ²²R. M. Macfarlane, *J. Chem. Phys.* **47**, 2066 (1967).
- ²³R. M. Macfarlane, *Phys. Rev. B* **1**, 989 (1970).
- ²⁴K. Zdzanski, *Phys. Rev.* **159**, 201 (1967).
- ²⁵S. Sugano, Y. Tanabe, and H. Kamimura, *Multiplets of Transition-Metal Ions in Crystals* (Academic, New York, 1970).
- ²⁶E. König and R. Schnakig, *Chem. Phys. Lett.* **32**, 553 (1975).
- ²⁷E. König and R. Schnakig, *Phys. Status Solidi B* **77**, 657 (1976).
- ²⁸E. König and R. Schnakig, *Phys. Status Solidi B* **78**, 543 (1976).
- ²⁹W. L. Yu and C. Rudowicz, *Phys. Rev. B* **45**, 9736 (1992).
- ³⁰C. W. Neilson and G. F. Koster, *Spectroscopic Coefficients for the p^n , d^n , and f^n Configurations* (MIT, Cambridge, MA, 1963).
- ³¹W. L. Yu, *Phys. Rev. B* **39**, 622 (1989).
- ³²W. L. Yu, *Phys. Rev. B* **41**, 9415 (1990).
- ³³W. L. Yu and T. Tan, *Phys. Rev. B* **49**, 3243 (1994).
- ³⁴M. L. Du and C. Rudowicz, *Phys. Rev. B* **46**, 8974 (1992).
- ³⁵E. Francisco and L. Pueyo, *Phys. Rev. B* **37**, 5278 (1988).
- ³⁶T. P. P. Hall, W. Hayes, R. W. H. Stevenson, and J. Wilkens, *J. Chem. Phys.* **38**, 1977 (1963).